Modelling Sea Ice Growth

Mark J. McGuinness*

Received Day December 2007; revised Day Month Year

Abstract

The freezing of water to ice is a classic problem in applied mathematics, involving the solution of a diffusion equation with a moving boundary. However, when the water is salty, the transport of salt rejected by ice introduces some interesting twists to the tale. A number of analytic models for the freezing of water are briefly reviewed, ranging from the famous work by Neumann and Stefan in the 1800s, to the mushy zone models coming out of Cambridge and Oxford since the 1980s. The successes and limitations of these models and remaining modelling issues, are considered in the case of freezing sea-water in the Arctic and Antarctic Oceans. A new, simple model which includes turbulent transport of heat and salt between ice and ocean is introduced and solved analytically, in two different cases — one that turbulence is given by a constant friction velocity, and the other that turbulence is buoyancy-driven and hence depends on ice thickness. Salt is found to play an important role, lowering interface temperatures, increasing oceanic heat flux, and slowing ice growth.

1 Introduction

The temperature at which sea-water freezes depends on its salinity. The saltier the brine, the lower the freezing point. When salinity is above the critical value of 24psu, the freezing point is below the temperature of maximum density, so that colder sea-water is heavier. Then cooler surface waters are heavier and overturn, mixing a region of ocean down to a critical depth (the pyncnocline). This region is cooled to near freezing, rather than just the surface waters.

*Department of Mathematical Sciences, KAIST, Taejon 305-701, South Korea
mailto:Mark.McGuinness@vuw.ac.nz

When cold air causes open sea-water to begin to freeze, many small ice crystals (frazil ice) form at the surface, stirred by wind, waves and currents [10, 13, 6]. This may be further complicated by the formation of agglomerations of crystals called pancake ice, which collide and raft. A large solid sheet of ice is typically formed when a critical thickness of about 10cm is reached [6]. Then those crystals that are oriented with the direction of most rapid growth near vertical become predominant as the ice thickens.

Salt is rejected by growing ice as a dense brine, but the brine cannot escape as rapidly as heat at the ice-ocean interface. This is due to the diffusivity of salt being much less than thermal diffusivity. Then the very cold salty interface leads to a cold fresher region nearby. As a consequence, while the actual ice-ocean interface is at freezing point, the region below the interface is below freezing point, creating an unstable situation — any ice that protrudes into the supercooled region grows faster. This leads to the dendritic growth of ice as fingers or plates down into the sea. These fingers and plates then bridge across, trapping brine in the ice-brine mixture. This constitutional supercooling causes the ice-ocean interface to be convoluted, with a gradual transition from water to a mixture of liquid (brine) and ice called a mushy zone [10, 7, 34, 35], rather than a sudden planar change from liquid to ice.

Cold air drives the freezing process, and snow on top can complicate it by decreasing conductive heat flow. There is radiative heat transfer between atmosphere and ice. The ocean is relatively warm, with turbulent currents, and in Antarctica near glacial ice shelves is occasionally slightly supercooled with billows of small ice crystals present, to further complicate the picture.

2 Previous Models

Classic work by Neumann in the 1860s [3] and famously Stefan in 1891 [13] was seminal in the early modeling of the growth of sea ice. The diffusion equation, resulting from conservation of heat, is solved in one dimension with a moving boundary between ice and ocean, in the case that the boundary is sharp and heat transport from ocean to ice is negligible. The freezing interface is found to move as the square root of time. Salt transport is ignored.

Conservation of energy leads to the heat conduction equation for the temperature $T(t, z)$ of the ice (°C), assuming the ice can be approximated as a one-dimensional sheet with planar interfaces with air and ocean, z is

elevation and t is time,

$$\frac{\partial T}{\partial t} = D\frac{\partial^2 T}{\partial z^2}\ , \quad D \equiv \frac{k_i}{\rho_i C_i} \tag{1}$$

where D is the thermal diffusivity of the ice (which averages about $10^{-6}\mathrm{m}^2.\mathrm{s}^{-1}$ over the temperature range -2 to -25°C for an ice salinity of 5 psu), $\rho_i \approx$ 910 kg.m^{-3} is the ice density, C_i its thermal capacity (J.kg^{-1}°C^{-1}), and $k_i \approx 2.2$ W.m^{-1}.K^{-1} its thermal conductivity [14, 25, 26]. Trapped brine means that C_i and D have a strong dependence on T [24, 25].

Boundary conditions used by Stefan and Neumann are that at the air-ice interface $z = 0$ the ice temperature T_0 is equal to the air temperature $T_a(t)$, and at the moving boundary $z = -h(t)$ that is the ice-ocean interface, the temperature is at freezing point T_f, and the latent heat removal that advances the freezing front at $\dot{h}$ m.s^{-1} is caused by heat conduction upwards to the colder air through the ice, so that

$$\rho_i L\dot{h} = -k_i \left.\frac{\partial T}{\partial z}\right|_{-h^+}\ , \tag{2}$$

where $L \approx 3.3 \times 10^5$ J.kg^{-1}.K^{-1} is the latent heat of fusion for sea-water.

The air temperature oscillates, and these temperature variations penetrate sea ice at rates (and to effective depths) dependent on frequency, with a phase velocity [3] estimated for constant diffusivity as $2D/\delta$ m.s^{-1} where δ is the penetration depth of the thermal wave. The slowest waves then penetrate with phase velocities $2D/h$ m.s^{-1}, which is faster than the ice growth rate estimated at $k_i(T_f - T_a)/(\rho_i L h)$ provided that

$$T_f - T_a < 2D\rho_i L/k_i \approx 300^\circ\ \mathrm{C}\ .$$

For air temperatures encountered in Antarctica and the Arctic, this inequality is easily satisfied. T_f is about -2°C depending on salinity, and T_a during freezing ranges from this value to about -70°C. This means that the slowest penetrating thermal waves do travel much faster than the ice growth rate. This does not mean that the temperature profile is always linear — observations indicate otherwise, and the observed curvature of temperature versus depth has been used to directly estimate the thermal conductivity of sea ice [14, 25, 26]. However, oscillations also damp out as they penetrate, with a damping factor of the order of $\exp(-\sqrt{\omega/(2D)}\,z)$ [3], where ω is the frequency of oscillation. Then, for example, an oscillation with period 40 days damps by a factor of e over a lengthscale of 1m, and smaller period oscillations damp out over even shorter depths. This suggests that a running

average of 40 days or so is a reasonable pre-treatment for air temperatures — the ice effectively averages out rapid changes. Such a running average has much less variability than the original air temperature.

For the purposes of calculating ice growth rate, a linear approximation (that is, a steady-state solution to Equation 1) is often used to estimate the average temperature gradient in the ice at the ice-ocean interface,

$$\frac{\partial T}{\partial z} \approx \frac{T_a - T_f}{h} \ ,$$

and the Stefan problem becomes

$$\dot{h} = \frac{k_i}{\rho_i L h}(T_f - T_a) \ . \tag{3}$$

This integrates to give the Stefan solution

$$h^2 = \frac{2k}{\rho_i L}\theta \approx 1.4 \times 10^{-8} \ \theta \ , \tag{4}$$

where $\theta \equiv \int_0^t (T_f - T_a) \ dt$ is the number of degree-seconds of cooling. For a constant air temperature θ is linear in time, so that h grows as the square root of time. The Stefan solution is graphed in Fig. 2, alongside data and later model results.

Stefan's solution is generally regarded as giving an upper limit on ice growth rate and thickness. Snow reduces heat flow, solar heating slows cooling, and heat flow from ocean to ice slows cooling — these effects have been ignored.

A more sophisticated boundary condition at the upper ice surface allows for a thermal boundary layer in the air, or for a layer of snow, so that there is a flux (or mixed boundary) condition,

$$\frac{\partial T}{\partial z} = \alpha(T_a - T_0) \ , \quad z = 0 \ , \tag{5}$$

where α is a nonnegative heat transfer coefficient with units m^{-1}, which depends on snow thickness if snow is present [21, 12]. This results in

$$\dot{h} = \frac{k\alpha}{\rho_i L(1 + \alpha h)}(T_f - T_a) \ , \tag{6}$$

which integrates to give

$$h^2 + \frac{2}{\alpha}h = \frac{2k}{\rho_i L}\theta \ . \tag{7}$$

In the limit $\alpha \to \infty$, the mixed boundary condition reduces to Stephan's condition $T_a = T_0$, and the solution for h reduces to the Stefan solution. In general for positive α, ice growth is slower that the square root of time Stefan behaviour, although for $\alpha = 40$ m^{-1} the graphs practically coincide (Fig. 2). Small α gives linear growth of h with θ, and zero α corresponds to a perfectly insulated upper boundary, with no heat taken from the ice and no ice generated.

An empirical fit [1] to the thickness of snow-free ice in Thule, Greenland, illustrated in Fig. 1 to show the scatter of data points, used the same formula,

$$h^2 + 0.051h = 0.775 \times 10^{-8}\,\theta \tag{8}$$

where h is in m, and θ is degree-seconds. See [22] for other empirical relationships.

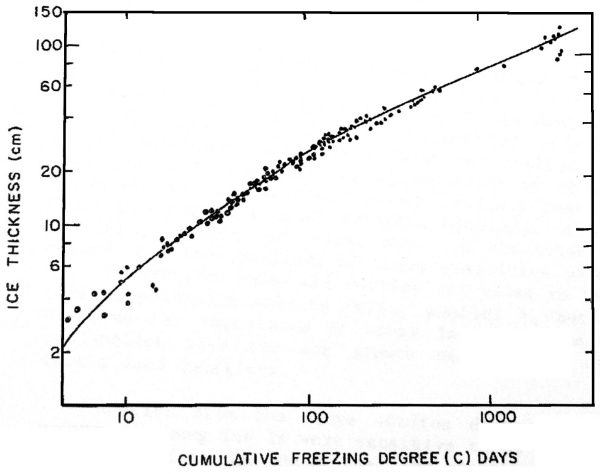

Figure 1: Data and empirical fit to snow-free ice near Greenland, after Anderson, 1961 [1]. *(Reprinted with permission of the International Glaciological Society and Prof. Anderson)*

Matching the coefficients of h in Equations 7 and 8 implies that $\alpha \approx 40$ m^{-1}. However, the constant term on the right-hand side of Equation 8 is not a good match with known values listed earlier in this paper. Fig. 2 shows a comparison between the empirical (data) thicknesses given by 8 and our solution 7, using $\alpha = 40\text{m}^{-1}$. Our simple model (with up-to-date values for k_i, ρ_i, and L) predicts a faster growth of sea ice than is observed.

Reducing our k_i value from 2.2 to 1.3 gives a good fit to the data (graphically indistinguishable from the fit that Anderson drew, Fig. 1), but this is at the cost of almost halving the typical measured value of thermal conductivity in sea ice [14]. A number of missing factors in the model could account for

the misfit, including radiative heat transfer, heat flow from the ocean to the ice (the oceanic heat flux), and the role played by the transport of salt. We will consider the latter two mechanisms in the next Section.

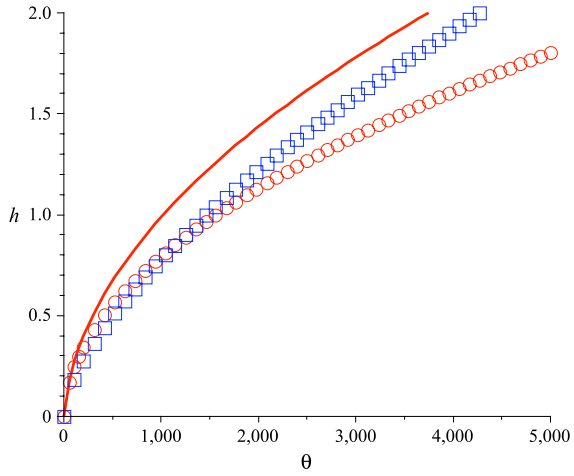

Figure 2: A graph of ice thickness h in m versus degree-days of cooling θ, comparing an empirical fit by Anderson [1] (circles), an empirical fit to data from McMurdo Sound [27] (boxes), and Stefan's solution and our simple model 7 with $\alpha = 40$, which both plot almost identically (solid line).

Also shown in Fig. 2 is a fit to sea ice thicknesses measured in McMurdo Sound [27]. These grow slower initially than Anderson's measurements, then faster once the ice is about 1m thick. This may be related to the appearance of a different ice crystal structure in the McMurdo ice [27] at this thickness, possibly associated with the accretion of ice from a supercooled mixed oceanic layer. Slow early solid ice growth may be due to heat transport from this layer, as it is supercooled, and later faster growth of solid ice may be reaping the benefit of small crystals of ice that are nucleated in the mixed layer, rising to the solid ice interface and sticking there.

A very detailed vertical model of the heat conduction problem is solved numerically by Maykut and Untersteiner [22]. They concentrate particularly on the interface between atmosphere and ice, and on parameterisations of the various mechanisms for heat exchange there, especially radiative transport. Salt transport is not modelled, however, which may impact on heat transport from the ocean.

3 Salt Transport

Here we consider the importance of also modelling the transport of salt, for the growth of sea ice. Salt alters the freezing point of sea-water, and salt diffusivity is very different to thermal diffusivity.

Weber [32] considers the very early growth of sea ice, and includes salt transport. He shows that the coupling between salinity and heat transport cannot be neglected. His model, like that of Stefan, ignores heat transport between ice and ocean. Salt transport to the ocean is modelled as diffusive. The model is solved by a heat balance integral method, which uses a polynomial approximation to the temperature and salinity profiles. Weber assumes a small temperature drop across the ice, and takes the interface to be sharp and smooth. Recent measurements and modelling suggest that all three of these assumptions are violated in practice (e.g., [6]) in the early growth of fresh polar sea ice.

Weber does find that including salt transport reduces ice growth rate, because salt lowers the freezing temperature at the ice-ocean interface, and for his thin ice this affects heat transport to the atmosphere. Furthermore, ice growth rate in his model is proportional to the square root of time, for constant air temperature. Weber notes that the rejected salt will lead to convection, and that morphological instability and dendritic ice growth is likely, invalidating the assumption of a flat interface between ice and ocean.

A similar approach is taken by Notz *et al* [23] in their modelling of the formation of a false bottom under summer melt ponds in the Arctic. Their model admits a similarity solution, since there are no external length or time-scales, and interfaces grow as the square root of time.

3.1 Turbulent Transport

The turbulent transport of heat and salt in the general context of cooling a binary alloy is modelled by Woods and Huppert [33]. They posit a boundary layer beneath the ice, and flux terms depending on a Rayleigh number to the power of one third. Various turbulent sub-models are considered, including the formation of plumes or blobs of brine, and various relative rates of transport of heat and salt are examined. Their mixed layer is of finite extent, and may become supercooled. Small-time asymptotic analysis gives square-root of time growth, which changes to linear in time behaviour later on, in the limit of relatively slow salt transport.

A new simple model that extends the Stefan approach to include the turbulent transport of heat and salt at the ice-ocean interface is now introduced here and solved approximately. A linear temperature profile in the ice is as-

sumed, with the surface of the ice at air temperature. Conservation of heat and salt at the growing interface gives

$$\dot{h} = \frac{k_i(T_f - T_a)}{\rho_i L h} - \frac{Q_T}{\rho_i L} \ , \tag{9}$$

and

$$\dot{h} = \frac{Q_S}{\mathcal{D}S} \ , \tag{10}$$

where $\mathcal{D}S = \rho_i(S_i - S_w)$, and Q_T and Q_S are turbulent fluxes of heat and salt.

We assume there is a thermal and saline boundary layer in the ocean next to the ice with density ρ_w, temperature T_f, and salinity S_w. The average salinity in the sea ice is S_i. Units for salinity are parts per thousand, or gms of salt per kg of brine. We assume that parts per thousand equates to the same number as psu (practical salinity units).

The average salinity of sea ice and of the ocean, near the ice-ocean interface, depend on how fast it is freezing. We model the variation of sea ice salinity by taking the salinity of sea ice to be proportional to the (variable) salinity of the sea-water near the ice (as in Schmidt *et al*, 2004), so that

$$S_i = f S_w \ , \quad \text{where } f \approx 0.14 \ ,$$

and hence,

$$\mathcal{D}S = -S_w \varrho_i (1 - f) \approx -0.86 S_w \varrho_i \ . \tag{11}$$

Freezing point is approximated as [32]

$$T_f = -A S_w \ , \tag{12}$$

where $A \approx 0.054$ °C/psu.

The turbulent flux terms for heat and salt are (using a simple model for transfer between a region close to the ice with salinity and density S_w and ϱ_w, to a well-mixed region further away):

$$Q_T = -C_H u_* (T_f - T_m) \varrho_w C_w \ , \tag{13}$$

and

$$Q_S = -C_S u_* (S_w - S_m) \varrho_m \ , \tag{14}$$

where the constants T_m, ϱ_m, and S_m are temperature, density, and salinity in a deeper, well-mixed ocean layer, C_w is the thermal capacity of that water,

and $C_H \approx 0.0058$ is a turbulent transfer coefficient measured in the field[17]. A value for C_S is here calculated from C_H in the spirit of [16] as

$$C_S = C_H \left(\frac{\mathrm{Pr}}{\mathrm{Sc}}\right)^{2/3} \approx 0.03 C_H \approx 2 \times 10^{-4} \ .$$

Here, Sc= 2432 is the Schmidt number for salt in water (kinematic viscosity divided by molecular diffusivity), and Pr= 13.4 is the Prandtl number (kinematic viscosity divided by thermal diffusivity). This parametrisation of the turbulent transport of salt and heat reflects the importance under ice of a viscous sublayer, across which molecular properties are significant [16], making the transport of salt comparatively slow.

We will use the simple average value for the friction velocity, $u_* \approx 0.015$ m/s, as measured in the Weddell Sea in 1996 [17], and take the mixed layer in the ocean to be at the freezing temperature for its salinity. Then our variables are ice thickness $h(t)$ and boundary-layer salinity $S_w(t)$. Equating the right-hand sides of Equations 9 and 10 gives a quadratic for S_w as a function of h,

$$S_a S_w^2 + S_b S_w + S_c = 0 \ , \tag{15}$$

where $S_a \equiv C_H u_* \rho_w C_w A/L + k_i A/(Lh)$, $S_b \equiv C_H u_* \rho_w C_w T_m/L + k_i T_a/(Lh) + C_s u_* \rho_m/0.86$, and $S_c \equiv -C_s u_* \rho_m S_m/0.86$. With an eye on Equation 10, it is useful to transform variables in Equation 15 as $Y = S_w/(S_w - S_m)$. The resulting quadratic in Y,

$$Y_a Y^2 + Y_b Y + S_c = 0 \ , \tag{16}$$

where $Y_a \equiv S_a S_m^2 + S_b S_m + S_c$ and $Y_b \equiv -(S_b S_m + 2S_c)$, has a solution that is closely matched by taking the balance between the Y^2 and the Y terms, giving a linear dependence on h,

$$Y \approx \frac{T_a}{AS_m + T_a} + \frac{u_*}{k_i}\left(\frac{C_H \rho_w C_w T_m - C_s \rho_m L/0.86}{AS_m + T_a}\right) h \approx 1 + Y_1 h \ , \tag{17}$$

where $Y_1 \approx -780/T_a$ for air temperatures much less than T_f.

Then if the air temperature T_a is taken to be constant, Equation 10 integrates to give the solution

$$h^2 + \gamma_1 h \approx \frac{2k_i}{\rho_i \mathcal{L}} \theta \ , \tag{18}$$

where $\gamma_1 \equiv 1.7 k_i |T_a|/(u_* C_s \rho_m \mathcal{L})$, and $\mathcal{L} \equiv L - \frac{0.86 C_H \rho_w C_w T_m}{C_s \rho_m}$. Using our parameter values this becomes

$$h^2 + \frac{|T_a|}{460} h \approx 0.88 \times 10^{-8} \ \theta \ , \tag{19}$$

which, using a range of air temperatures, $T_a = -5$ to $-45°$C, gives a close match to Anderson's data as illustrated in Fig. 3.

The term γ_1 reflects the effect of salt transport on ice growth, and vanishes as $C_s u_* \to \infty$ and salt transport increases. If $C_s \to \infty$, then $\mathcal{L} \to L$ and Stefan's solution is recovered. If C_s vanishes, h becomes linear in θ and also vanishes.

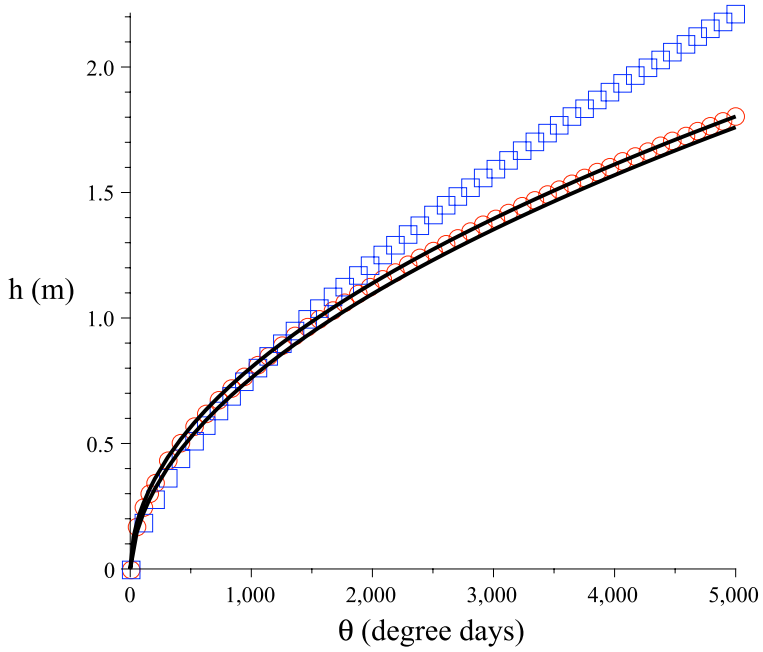

Figure 3: Data from Anderson [1] (circles), Purdie *et al* [27] (boxes), and our turbulent salt transport model 19 with $T_a = -5°$C (upper curve) and $T_a = -45°$C (lower curve).

Note that salt transport has considerably reduced the modelled ice growth rate. Other authors have noted the importance of including salt transport, although in different contexts [23, 32] to the present one. Here, salt can be understood to be a bottle-neck in the transport process, accumulating in our model at the ice-ocean interface because it has a much smaller diffusivity than heat. The heat balance is satisfied because the accumulation of salt lowers the ice temperature there, and increases the oceanic heat flux to the ice (commensurate with a slower growth rate).

The heat flux from the freezing interface to the air, and the heat flux from the ocean to the freezing interface, are graphed in Fig. 4, assuming an air temperature of -25°C. These values compare well with measured values in polar waters [17]. The oceanic heat flux is significant compared with the

heat flux to the atmosphere, which is about 2.6 times the oceanic heat flux.

The ratio of oceanic and atmospheric heat fluxes is almost constant over the ice thickness range 0.1–2 m. This is because both fluxes depend approximately on the inverse of ice thickness h, the flux to air because the average temperature gradient is inversely proportional to h, and the oceanic heat flux because the salinity and hence the freezing temperature at the interface is roughly inversely proportional to h.

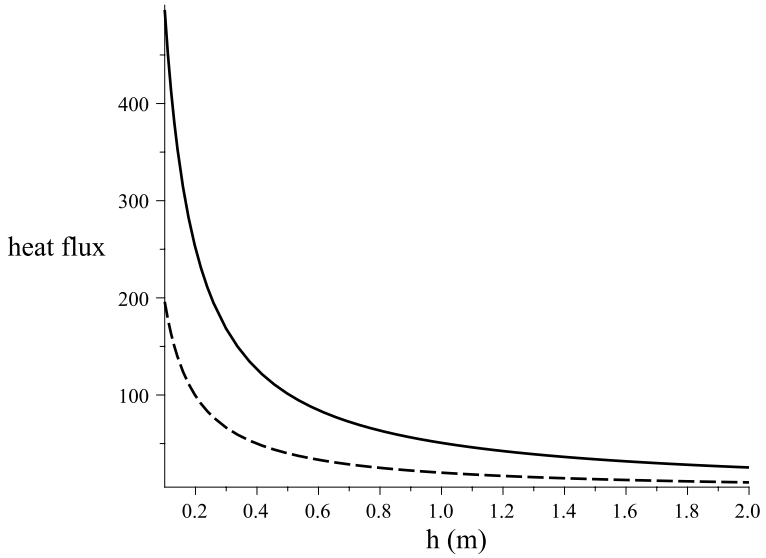

Figure 4: Heat fluxes (W.m^{-2}) from freezing ice-ocean interface to air (upper curve) and from the ocean to that interface (lower curve), versus ice thickness, for the turbulent transport model with constant friction velocity and an air temperature of -25°C. The net heat flux from the freezing front is the difference between these two fluxes.

3.2 Buoyancy driven turbulence

The previous model used a constant friction velocity that reflected an average turbulence environment consistent with field measurements. However, one of the factors driving turbulent transport is the rejection of brine from growing sea ice in turbulent plumes. Since brine is rejected more rapidly when ice is growing faster, there is a coupling between friction velocity and ice growth rate. Now we consider the effects of taking turbulent transport to be driven entirely by brine rejection.

This may be modelled [2, 8, 19, 31] by taking $u_* = \sqrt{C_d}\, W_*$, where $C_d \approx 1.3 \times 10^{-3}$ is the drag coefficient [9], and W_* is the Deardorff or free

convection velocity scale [5]. Turner [30] gives W_* in terms of the buoyancy flux

$$W_*^3 = B\lambda \, , \tag{20}$$

where the buoyancy flux is $B \equiv -\frac{g\langle \varrho'_w w' \rangle}{\langle \varrho_m \rangle}$ (see also [18]), and $\langle \varrho'_w w' \rangle$ is the average vertical flux (positive upwards in this paper) of random variations ϱ'_w in fluid density at the ice-ocean interface, and $\langle \varrho_m \rangle$ is the mixed layer density. The lengthscale used is [18] $\lambda = \kappa z_i$ where $\kappa = 0.4$ is von Kármán's constant. The term z_i is the thickness of the mixed layer, stirred by brine rejection under the growing sea ice, and from measurements [11] is of the order of 50m in mid-winter in McMurdo Sound. Fluid density depends mainly on salinity, so that

$$\frac{d\varrho_w}{dS} \equiv \varrho_{ws} \approx 0.81 \text{ kg/m}^3\text{/psu}$$

and $\varrho'_w = \varrho_{ws} S'_w$. Then $B \approx -\frac{\varrho_{ws}\, g\langle w' S'_w \rangle}{\langle \varrho_m \rangle}$. The average vertical flux of salt follows from our model, using Equation 10:

$$\langle w' S'_w \rangle = \dot{h} \, \frac{\mathcal{D}S}{\varrho_w} \approx -\frac{0.86 \, \dot{h} \, S_w \varrho_i}{\varrho_w} \, . \tag{21}$$

Hence,

$$W_*^3 = 0.86 \, \varrho_{ws} \, \lambda g \dot{h} \left(\frac{S_w \varrho_i}{\varrho_m \varrho_w} \right) \, . \tag{22}$$

Then the friction velocity may be found in terms of salinity in the boundary layer from the model equations, $u_* = C_d^{3/4} \sqrt{b(S_w - S_m)}$ and $W_* = u_*/\sqrt{C_d}$, where $b \equiv \lambda g C_S \varrho_{ws}/(0.86 \, \varrho_w)$.

Equating the right-hand sides of Equations 9 and 10 then gives a quintic in $\Delta S \equiv \sqrt{S_w - S_m}$. The physically realistic solution to this quintic is approximated within 10% by matching the cubic and constant terms, to get a linear relationship between ΔS and $h^{-1/3}$. Substituting this back into Equation 10 gives

$$\dot{h} \approx \frac{k_i |T_a|}{\rho_i L \gamma_3 (h + \gamma_2 h^{\frac{1}{3}})} \, , \tag{23}$$

where

$$\gamma_2 \equiv \left(\frac{0.86 \, k_i |T_a|}{\gamma_3 C_s \rho_m L C_d^{3/4} \sqrt{b S_m}} \right)^{\frac{2}{3}}$$

and

$$\gamma_3 \equiv 1 - \frac{0.86 \, C_H \rho_w C_w T_m}{C_S \rho_m L} \, .$$

This integrates for constant T_a, giving

$$h^2 + \frac{3}{2}\gamma_2 h^{\frac{4}{3}} = \frac{2k_i}{\rho_i L \gamma_3}\theta \; . \tag{24}$$

The term γ_2 is of order C_s^{-1}, so vanishes as salt transport increases, recovering Stefan's solution, and γ_2 is singular as salt transport reduces to zero, giving similar behaviour to the previous model which assumed constant u_*. The solution given by Equation 24 is graphed in Fig. 5 for the case that air temperature is -25°C, and compared with data and the previous model.

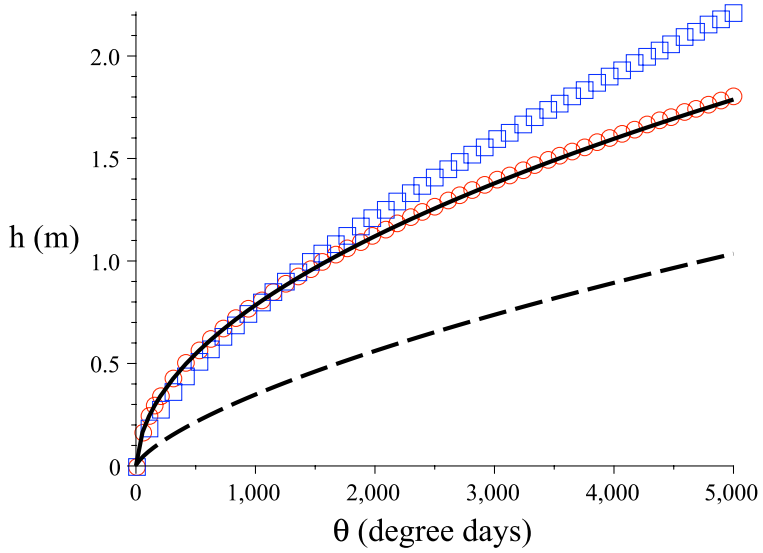

Figure 5: Data from Anderson [1] (circles), Purdie *et al* [27] (boxes), a constant turbulence salt transport model 19 with $T_a = -25°\mathrm{C}$ (solid curve) and a model with only buoyant plumes driving the turbulence (dashed curve) as in Equation 24, also with $T_a = -25°\mathrm{C}$.

The modelled ice thickness when turbulence is driven by buoyancy is much less than data and other models indicate. This is because of the assumption that only buoyancy, from rejected brine plumes, drives turbulence under sea ice. Typical values of u_* obtained from this model are about one hundred times smaller than the measured value 1.5×10^{-2} m.s^{-1} used in the previous model. This suggests that brine rejection plays a minor role in generating turbulence in the mixed layer. So in this model, salt builds up at the ice-ocean interface, lowering the temperature there. The result is a much increased oceanic heat flux to the freezing interface, and hence a much reduced net heat flux from it. Relatively more heat is removed from the oceanic mixed layer, at the expense of the growth of the freezing front.

Both turbulent salt flux models predict cooling of the oceanic mixed layer by this mechanism, which may lead to supercooling. It is unclear how supercooling in the mixed layer is relieved — ice may grow in dendritic structures from the interface, especially if supercooling is greater nearby, and/or ice may grow from nucleation sites within the turbulent mixed layer. The latter mechanism is a relatively efficient way to make ice, in the form of turbulent billows of small ice crystals [11, 20] within the mixed layer, as this ice does not immediately thicken the layer of solid ice. Hence heat flow to the atmosphere is more rapid than if the ice does thicken this layer.

A dendritic response to supercooling means the interface between ice and ocean is not planar but highly convoluted. One modelling approach to this phenomenon is to approximate such a mushy zone as a porous medium made of ice and brine, with a porosity and permeability that depend on temperature [33, 34, 35, 36, 7]. The ice-ocean boundary is then warmer than in the planar interface models with salt transport, and oceanic heat flux is reduced.

4 Conclusions

The inclusion of salt transport is important when modelling the growth of sea ice. A simple model for turbulent transport of salt and heat between ice and ocean characterised by a constant friction velocity has been developed and solved. In this model, the presence of salt at the ice-ocean interface lowers the freezing temperature there, increasing the heat flux from the ocean, and slowing down the growth of sea ice, to give an excellent match with observations.

While the modelling of the growth of sea ice has come a long way since the remarkable work of Neumann and Stefan, it still falls short of modern understandings of ice structure and oceanic conditions. The constant friction velocity model presented here does well in fitting Anderson's classic data, and is consistent with observed oceanic heat fluxes, but fails to explain changes in ice crystal structure often seen in thicker sea ice [28, 29].

Mushy zone models are a good approach to modelling the dendritic growth observed in supercooled waters, but do not address the question of which ice growth mechanism will dominate in a supercooled ocean under sea ice — dendritic growth from solid surface ice, or frazil growth from nucleation sites within a turbulent oceanic mixed layer. Models addressing such frazil growth will have to contend with the growth and breakage of a population of small discs of ice with a size distribution [4], rising under buoyancy but stirred by turbulence, stabilising the turbulence by buoyancy, and interacting with the

temperature and turbulence fields and with the solid ice above.

Acknowledgements: The author would like to thank Pat Langhorne at the University of Otago in New Zealand, and Mike Williams at the National Institute of Water and Atmospheric Research in New Zealand, for many useful discussions and for data; and the Marsden Fund of New Zealand and Victoria University of Wellington in New Zealand for financial support.

References

[1] Anderson, D.L. Growth rate of sea ice, *J. Glaciol.* **3**, 1961, 1170–1172.

[2] Beljaars, A.C.M., The parameterization of surface fluxes in large-scale models under free convection, *Quart. J. Roy. Met. Soc.* **121**, 1995, 255–270.

[3] Carslaw, H.S., & Jaeger, J.C. *Conduction of heat in solids*, Oxford University Press, Oxford, 1959.

[4] Daly, S.F., *Frazil Ice Dynamics*, CRREL Monograph **84-1**, Hanover NH, 1984.

[5] Deardorff, J.W., Convective Velocity and Temperature Scales for the Unstable Planetary Boundary Layer and for Rayleigh Convection, *J. Atmos. Sci.* **27**, 1970, 1211–1213.

[6] Eicken, H. From the microscopic, to the macroscopic, to the regional scale: Growth, microstructure and properties of sea ice, Chapter 2, *Sea Ice An introduction to its physics, chemistry, biology and geology*, Editors Thomas, D.N., & Dieckmann, G.D., Blackwell Publishing, Oxford, UK, 2003.

[7] Fowler, A.C. The formation of freckles in binary alloys, *IMA Journal of Applied Mathematics* **35**, 1985, 159–174.

[8] Grachev, A.A., Fairall, C.W. , and Larsen, S.E. On the determination of the neutral drag coefficient in the convective boundary layer, *Boundary Layer Meteorol.* **86** , 1998, 257–278.

[9] Holland, D.M., & Jenkins, J.A. Modelling thermodynamic ice-ocean interactions at the base of an ice shelf, *J. Phys. Oceanogr.* **29**, 1999, 1787–1800.

[10] Lake, R.A., & Lewis, E.L. Salt rejection by sea ice during growth, *J. Geophys. Res.* **75**, No. 3, 1970, 583–598.

[11] Leonard, G.H., Purdie, C.R., Langhorne, P.J., Haskell, T.G., Williams, M.J.M., & Frew, R.D. Observations of platelet ice growth and oceanographic conditions during the winter of 2003 in McMurdo Sound, Antarctica, *J. Geophys. Res.* **111**: C04012, 2006, `http://dx.doi.org/10.1029/2005JC002952`.

[12] Lepparanta, M. A review of analytical models of sea-ice growth, *Atmosphere-Ocean* **31**(1), 1993, 123–138.

[13] Lock, G.S.H. *The growth and decay of ice*, Cambridge University Press, 2005.

[14] McGuinness, M.J., K. Collins, H.J. Trodahl, & T.G. Haskell, Nonlinear thermal transport and brine convection in first year sea ice, *Ann. Glaciol.* **27**, 1998, 471–476.

[15] McGuinness, M.J. & Landman, K. Mean Action Time for Diffusive Processes, *Journal of Applied Mathematics and Decision Sciences* **4**(2), 2000, 125–141.

[16] McPhee, M.G., Maykut, G.A., & Morison, J.H., Dynamics and thermodynamics of the ice/upper ocean system in the Marginal Ice Zone of the Greenland Sea, *J. Geophys. Res.* **92** (C7), 1987, 7017–7031.

[17] McPhee, M.G., Kottmeier, C., & Morison, J.H., Ocean heat flux in the central Weddell Sea during winter, *J. Phys. Oceanogr.* **29**, 1999, 1166–1179.

[18] McPhee, M.G., & Morison, J.H. Under-Ice Boundary Layer, in *Encyclopedia of Ocean Sciences*, Academic Press, London, 2001, 3071–3078. `http://dx.doi.org/10.1006/rwos.2001.0146`

[19] Mahrt, L., D. Vickers, J. Edson, J. Sun, J. Højstrup, J. Hare, & J.M. Wilczak, J.M., Heat flux in the coastal zone, *Boundary Layer Meteorol.* **86**, 1998, 421–446.

[20] Martin, S. Frazil ice in rivers and oceans, *Ann. Rev. Fluid Mech.* **13**, 1981, 379–397.

[21] Maykut, G.A. The surface heat and mass balance, Chapter 5 in *The Geophysics of Sea Ice*, edited by N. Untersteiner, pp. 395–465, Plenum, New York, 1986.

[22] Maykut, G.A., & Untersteiner, N. Some results from a time-dependent, thermodynamic model of sea ice, *Jour. Geophys. Res.* **76**, 1971, 1550–1575.

[23] Notz, D., McPhee, M.G., Worster, M.G., Maykut, G.A., Schlünzen, K.H., & Eicken, H. Impact of underwater-ice evolution on Arctic summer sea ice, *Jour. Geophys. Res.* **108**(C7), 2003, 3223. `http://dx.doi.org/10.1029/2001JC001173`

[24] Ono, N. Thermal properties of sea ice, IV, Thermal constants of sea ice, *Low Temperature Sci.* **A26**, 1968, 329–349.

[25] Pringle, D., Trodahl, J.H., & Haskell, T. Direct measurement of sea ice thermal conductivity: No surface reduction, *J. Geophys. Res.* **111**, 2006, C05020, `http://dx.doi.org/10.1029/2005JC002990`.

[26] Pringle, D.J., Eicken, H. J. Trodahl, & H.J., Backstrom. L.G.E. Thermal conductivity of landfast Antarctic and Arctic sea ice, *J. Geophys. Res.* **112**, 2007, C04017, `http://dx.doi.org/10.1029/2006JC003641`.

[27] Purdie, C, Langhorne, P., Leonard, G., & Haskell, T. Growth of first year land-fast Antarctic sea ice determined from winter temperature measurements, *Annals of Glaciology* **44**, Number 1, November 2006 , 170–176.

[28] Smith, I.J., Langhorne, P.J., Trodahl, H.J., Haskell, T.G. and Cole, D.M., *Platelet ice - the McMurdo Sound Debate*, in H.T. Shen, ed., *Ice in Surface Waters - Proceedings of the 14th IAHR Symposium on Ice*, A.A. Balkema, Rotterdam, Netherlands, 1999, pp. 371–378.

[29] Smith, I.J., Langhorne, P.J., Trodahl, H.J., Haskell, T.G., Frew, R. and Vennell, R. Platelet ice and the land-fast sea ice of McMurdo Sound, Antarctica, *Annals of Glaciology* **33**, 2001, 21–27.

[30] Turner, J.S., *Buoyancy Effects in Fluids*, Cambridge University Press, in the series *Cambridge Monographs on Mechanics and Applied Mathematics,* Editors Turner, J.S., S. Davis, V. Tvergaard, G.K. Batchelor, & S. Leibovitch, 1979.

[31] Van den Hurk, B.J.J.M., & Holtslag, A.A. On the bulk parameterization of surface fluxes for various conditions and parameter ranges, *Boundary Layer Meteorol.* **82**, 1997, 119–134.

[32] Weber, J.E. Heat and salt transfer associated with formation of sea-ice, *Tellus* **29**, 1977, 151–160.

[33] Woods, A.W., & Huppert, H.E. The growth of a compositionally stratified solid above a horizontal boundary, *J. Fluid Mech.* **199**, 1989, 29–53.

[34] Worster, M.G. Solidification of an alloy from a cooled boundary, *J. Fluid Mech.* **167**, 1986, 481–501.

[35] Worster, M.G. Convection in mushy layers, *Annual Rev. Fluid Mech.* **29**, 1997, 91–122.

[36] Worster, M.G., & Wettlaufer, J.S. Natural convection, solute trapping, and channel formation during solidification of saltwater, *J. Phys. Chem.* **101**, 1997, 6132–6136.